PROCEEDINGS OF SCIENCE

Large-scale simulations with chiral symmetry

JLQCD Collaboration: T. Kaneko[*a,b†] **S. Aoki**[c]**, G. Cossu**[a]**, H. Fukaya**[d]**,**
S. Hashimoto[a,b]**, J. Noaki**[a]

[a] *High Energy Accelerator Research Organization (KEK), Ibaraki 305-0801, Japan*
[b] *School of High Energy Accelerator Science, The Graduate University for Advanced Studies (Sokendai), Ibaraki 305-0801, Japan*
[c] *Yukawa Institute for Theoretical Physics, Kyoto University, Kyoto 606-8502, Japan*
[d] *Department of Physics, Osaka University, Osaka 560-0043, Japan*

We carry out a comparative study among five-dimensional formulations of chirally symmetric fermions about the algorithmic performance, chiral symmetry violation and topological tunneling to find a computationally inexpensive formulation with good chiral symmetry. With our choice of the lattice action, we have launched large-scale simulations on fine lattices aiming at a precision study of light and heavy quark physics. We report on the comparative study, current status of the large-scale simulations, and preliminary results on the residual quark mass and auto-correltion.

31st International Symposium on Lattice Field Theory - LATTICE 2013
July 29 - August 3, 2013
Mainz, Germany

*Speaker.
†E-mail: takashi.kaneko@kek.jp

PoS(LATTICE 2013)125

1. Introduction

In the last several years, we performed an extensive study of QCD vacuum and light hadron physics by using the overlap action which exactly preserves chiral symmetry [1]. Our next target is a precision study of heavy flavor physics in collaboration with flavor factory experiments, such as the SuperKEKB / Belle II experiment, for a stringent test of the Standard Model.

Since the overlap action is computationally too expensive to simulate small lattice spacings $a \ll m_c^{-1}$ on reasonably large lattices, we carried out a systematic comparative study of a class of five-dimensional formulations that approximately satisfy the Ginsparg-Wilson relation to construct a computationally cheap formulation with good chiral symmetry. In this article, we report on the comparative study and the status of the on-going large-scale simulations with our choice of the lattice action.

2. Comparative study

We test five-dimensional fermion formulations [2] in this comparative study. The four-dimensional effective Dirac operator is given by

$$\frac{1+m_q}{2} + \frac{1-m_q}{2}\gamma_5\,\varepsilon_M\,(H_M)\,, \tag{2.1}$$

where the Hermitian kernel operator H_M and the approximation of its sign function ε_M can be chosen by tuning parameters appearing in the five-dimensional Dirac operator. Popular choices of H_M are the Wilson kernel $H_W = \gamma_5 D_W$, where D_W is the Wilson-Dirac operator, for the overlap fermions, and the Shamir kernel $H_T = \gamma_5 D_W/(2+D_W)$ for the standard domain-wall fermions. We also test a scaled Shamir kernel $2H_T$ [2]. While $2H_T$ has the same condition number as H_T, its low-lying eigenvalues are scaled up by a factor of 2. These kernels are combined with the Zolotarev (ε_Z) and polar decomposition (ε_p) approximations. By applying up to 6 level stout smearing [3] ($N_{\rm smr} = 0, 3, 6$), we test 8 different formulations listed in Table 1.

Table 1: Simulation setup in our comparative study. The first three columns show our choices of the five-dimensional formulation: the number of smearing $N_{\rm smr}$, kernel operator H_M and sign function approximation ε_M. We also list simulation parameters, namely β and the bare quark mass in lattice units am_{ud}, as well as results for a^{-1} and M_π.

$N_{\rm smr}$	H_M	ε_M	β	a^{-1} [GeV]	am_{ud}	M_π [MeV]
0	H_W	ε_Z	4.27	1.98(6)	0.0095, 0.0060, 0.0035	463(17), 375(17), 346(25)
0	H_T	ε_Z	4.11	1.92(6)	0.0200, 0.0120, 0.0065	543(18), 419(15), 318(15)
0	H_T	ε_p	4.11	1.97(5)	0.0200, 0.0090, 0.0040	623(19), 483(16), 400(15)
0	$2H_T$	ε_p	4.11	1.94(6)	0.0200, 0.0120, 0.0065	554(18), 434(17), 356(16)
3	H_W	ε_Z	4.29	1.94(6)	0.0145, 0.0090, 0.0050	472(18), 401(17), 330(17)
3	H_T	ε_p	4.18	2.00(8)	0.0250, 0.0170, 0.0090	534(23), 423(20), 374(23)
3	$2H_T$	ε_p	4.18	2.06(9)	0.0250, 0.0170, 0.0090	524(24), 469(24), 364(25)
6	$2H_T$	ε_p	4.18	2.11(6)	0.0250, 0.0170, 0.0090	511(17), 430(16), 337(20)

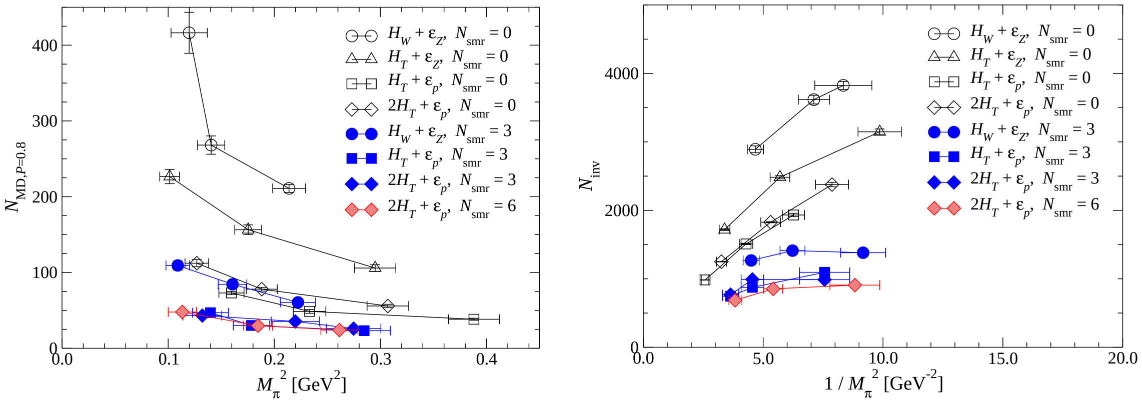

Figure 1: Left panel: number of MD steps $N_{\mathrm{MD},P=0.80}$ to attain 80 % acceptance rate. Data for different formulations are plotted in different symbols as a function of M_π^2. Right panel: CG iteration count N_{inv} as a function of M_π^{-2}.

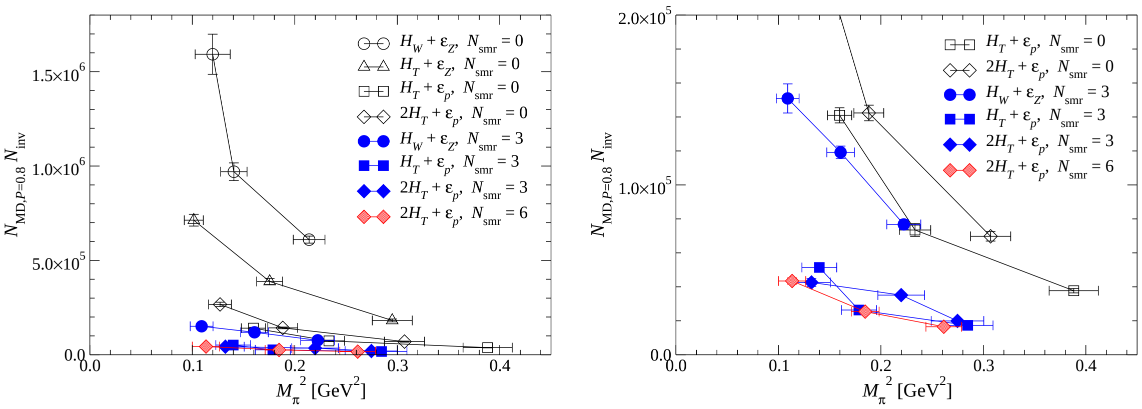

Figure 2: A measure of CPU cost per HMC trajectory $N_{\mathrm{MD},P=0.80}\,N_{\mathrm{inv}}$. The left panel shows all data, whereas the right panel is an enlargement of a region of small $N_{\mathrm{MD},P=0.80}\,N_{\mathrm{inv}}$ to focus on computationally cheaper formulations.

We carry out numerical simulations of two-flavor QCD by using these formulations and the tree-level Symanzik gauge action to study the performance of the Hybrid Monte Carlo (HMC) algorithm, chiral symmetry violation and topological tunneling. On a $16^3\times 32$ lattice, we simulate three pion masses in the range of $300 \lesssim M_\pi[\mathrm{MeV}] \lesssim 600$ at a single lattice cut-off around $a^{-1}\simeq$ 2 GeV. The fifth dimensional size is set to $N_5=12$. We set the range of the Zolotarev approximation $\varepsilon_Z(x)$ to $x\in[0.2,7.0]$ ($[0.4,7.0]$) for H_W without (with) smearing, and $[0.1,1.5]$ for H_T. Our statistics are 1,000 trajectories in each simulation. Parameters and results for a^{-1} and M_π are summarized in Table 1, where $r_0=0.462(11)(4)$ fm [4] is used as input to fix a.

In each simulation, we keep the acceptance rate of $P\simeq 0.7-0.9$ using a moderately small step size $\Delta\tau$ for the Molecular Dynamics (MD) integration. The number of the MD steps to attain a reference value $P=0.8$, which is denoted by $N_{\mathrm{MD},P=0.80}$ in the following, is estimated from the relations holding at small $\Delta\tau$

$$P=\mathrm{erfc}\left(\frac{1}{2}\sqrt{\langle\Delta H\rangle}\right), \qquad \langle\Delta H\rangle \propto \Delta\tau^4, \tag{2.2}$$

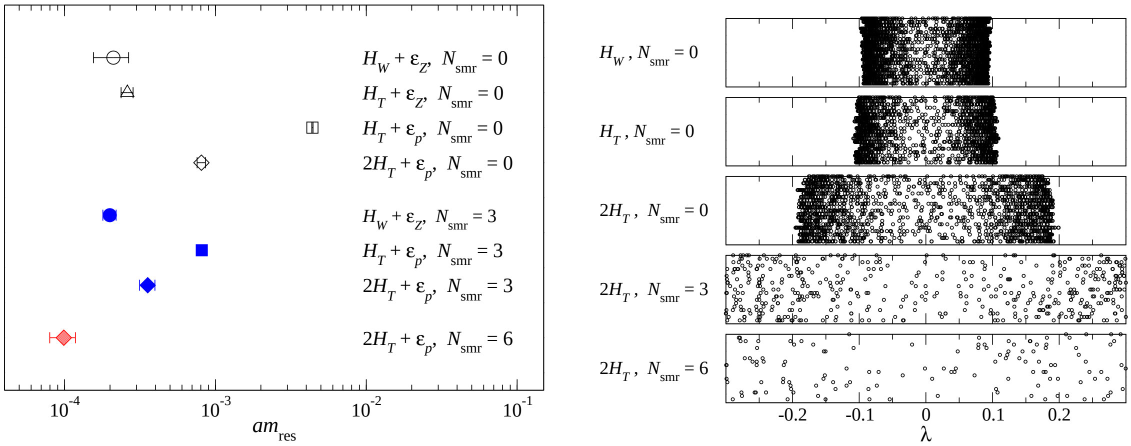

Figure 3: Left panel: a comparison of bare residual quark mass in lattice units, $am_{\rm res}$. Right panels: distribution of eigenvalue λ for several choices of the kernel operator. Note that we only plot the lowest 100 – 150 eigenvalues for thin-link kernels ($N_{\rm smr}=0$).

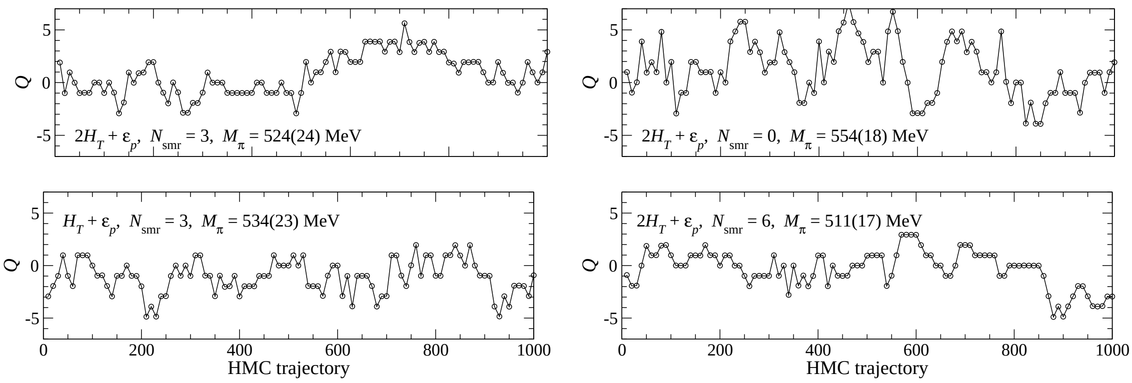

Figure 4: Monte Carlo history of topological charge. Left panels compare data for the Shamir-type kernels ($2H_T$ and H_T) with ε_p and $N_{\rm smr}=3$, whereas right panels show data for $2H_T$ with different $N_{\rm smr}$ (0 and 6).

where $\langle \Delta H \rangle$ represents the Monte Carlo average of the change of the Hamiltonian due to the discretized MD integration. Figure 1 compares $N_{{\rm MD},P=0.80}$ and the iteration count for CG per MD step, denoted by $N_{\rm inv}$, among the tested formulations. We observe that these two measures of the CPU cost significantly decrease by i) switching from H_W to $(2)H_T$, ii) switching from ε_Z to ε_p, and iii) applying smearing ($N_{\rm smr} \geq 3$). On the other hand, there is no large difference in these measures between Shamir-type kernels (H_T and $2H_T$) and between $N_{\rm smr}=3$ and 6.

The product $N_{{\rm MD},P=0.80} N_{\rm inv}$ can be considered as a measure of the CPU cost per HMC trajectory. As plotted in Fig. 2, the overlap formulation, namely the combination of H_W and ε_Z, turns out to be computationally very demanding. We can achieve about a factor of 20 acceleration at $M_\pi \simeq 400$ MeV: a factor of 5 by using $(2)H_T$ and ε_p, and an additional factor of 4 by smearing. We may expect even bigger gain at smaller quark masses.

These computationally cheaper formulations are, however, off from practical use, if they largely violate chiral symmetry. We compare residual quark mass $m_{\rm res}$ in Fig. 3. Since the min-max approximation can satisfy $|\varepsilon_Z(x)|^2 \sim 1$ in its approximation range, ε_Z leads to the least $m_{\rm res}$ at a given $N_{\rm smr}$. With our choice of $N_5=12$, however, $|\varepsilon_p(x)|^2$ largely deviates from unity at $x \lesssim 0.3$,

Table 2: Status of our simulations at $a^{-1} \simeq 2.4$ GeV. The third column shows the choice of the MD integrator, namely the leap-frog (LF) or Omelyan (O) integrator. We also list time per HMC trajectory on the whole machine of BlueGene/Q at KEK in the last column.

am_{ud}	am_s	MD	$N_{\rm MD}$	traj	P	$\langle \Delta H \rangle$	$\langle e^{-\Delta H} \rangle$	min/traj
0.019	0.040	LF	10	3000	0.78(1)	0.19(1)	0.99(1)	2.7
0.012	0.040	LF	13	2000	0.78(1)	0.17(1)	1.00(1)	3.5
0.012	0.040	O	3	1000	0.89(1)	0.07(2)	1.01(1)	2.0
0.007	0.040	LF	16	1000	0.74(1)	0.23(2)	1.04(3)	4.4
0.007	0.040	O	4	2000	0.90(1)	0.06(1)	1.00(1)	2.6
0.019	0.030	LF	10	3000	0.79(1)	0.17(1)	1.00(1)	2.8
0.012	0.030	LF	13	2000	0.79(1)	0.14(1)	1.02(2)	3.6
0.012	0.030	O	3	1000	0.88(1)	0.10(3)	1.00(2)	2.0
0.007	0.030	LF	16	2000	0.72(1)	0.27(2)	1.00(2)	4.5
0.007	0.030	O	4	1000	0.89(1)	0.08(2)	0.99(1)	2.6

where thin-link kernels have many low-lying modes as shown in Fig. 3. Scaling of the kernel $(H_T \rightarrow 2H_T)$ and smearing $(N_{\rm smr} = 3)$ are very effective to suppress these low-lying modes leading to an order of magnitude smaller $m_{\rm res}$ compared to the standard domain-wall fermions. Larger $N_{\rm smr}$ is better in reducing $m_{\rm res}$ but may distort short distance physics. We refer to Ref. [5] for more detailed discussions.

Figure 4 shows examples of the Monte Carlo history of the topological charge Q. A low-lying eigenvalue flips its sign along a tunneling between topological sectors. While scaling and smearing suppress the low-lying modes, the comparison in Fig. 4 suggests that these techniques do not prevent the topological tunneling at $a^{-1} \simeq 2$ GeV.

From this comparative study, we conclude that the combination of $2H_T$ and ε_p with $N_{\rm smr} = 3$ is the best choice among the tested formulations.

3. Large-scale simulations

We have launched large-scale simulations of $N_f = 2+1$ QCD with good chiral symmetry, namely with $m_{\rm res}$ well below the physical up and down quark mass $m_{ud,\rm phys}$. The tree-level Symanzik gauge action is combined with the fermion formulation chosen by the comparative study to be consistent with our $O(a^2)$-improvement program for heavy quark physics [6]. For controlled continuum and chiral extrapolations, we are planning to simulate the pion masses of 500, 400, 300 MeV (and even smaller) at four values of the lattice cut-off $a^{-1} \simeq 2.4$, 3.0, 3.6 and 4.8 GeV. Finite volume effects are suppressed to $1-2$ % level by keeping $M_\pi L \gtrsim 4$. These simulations are being carried out on BlueGene/Q at KEK (6 racks with a peak speed of 1.258 PFLOPS).

Table 2 shows the current status of our simulations on a $32^3 \times 64 \times 12$ lattice at $\beta = 4.17$, where a^{-1} determined from r_0 is expected to be $\simeq 2.4$ GeV. The three values of the bare light quark mass m_{ud} correspond to $M_\pi \approx 500$, 400 and 300 MeV, whereas we take two strange quark masses (m_s's) near its physical value $m_{s,\rm phys}$. We employ the Hasenbusch preconditioning [7] with the mass parameter $am' = 0.150$ for two degenerate light flavors, and the rational HMC algorithm [8] for the

Table 3: Status of our simulations at $a^{-1} \simeq 3.6$ GeV.

am_{ud}	am_s	am'	$N_{\rm MD}$	traj	$P_{\rm HMC}$	$\langle \Delta H \rangle$	min/traj
0.0120	0.0250	0.10	4	430	0.84(2)	0.10(2)	3.6
0.0080	0.0250	0.08	4	330	0.85(2)	0.06(2)	4.2
0.0042	0.0250	0.04	4	235	0.92(3)	0.04(2)	5.9
0.0120	0.0180	0.10	4	–	–	–	–
0.0080	0.0180	0.08	4	260	0.86(1)	0.05(1)	4.3
0.0042	0.0180	0.04	4	280	0.86(3)	0.02(2)	6.0

single strange flavor. We had started our simulations with the simple leap-frog MD integrator, which was later switched to the Omelyan integrator [9] leading to a factor of 2 speed-up. We keep reasonably high acceptance rate $P \simeq 0.7-0.9$ and confirm that $\langle e^{-\Delta H} \rangle = 1$ derived from the area preserving property of HMC is well satisfied.

We are also carrying out simulations at a larger lattice cut-off $a^{-1} \simeq 3.6$ GeV ($\beta = 4.35$) on $48^3 \times 96 \times 8$. The current status is summarized in Table 3. We increase the unit trajectory length to $\tau = 2$ based on our preparatory study on the auto-correlation (see below). Our choice of the fermion action as well as careful tuning of m' at each m_{ud} enable us to achieve the high acceptance rate $P \gtrsim 0.85$ with small $N_{\rm MD} = 4$. We expect half a year to accumulate 10,000 MD time on this large volume by using BlueGene/Q at KEK. This will be accelerated by further optimization of our simulation code [10].

We plot $m_{\rm res}$ from these simulations in Fig. 5, where the renormalization factor to the $\overline{\rm MS}$ scheme at 2 GeV is roughly estimated by matching our estimate of the bare value of $m_{s,\rm phys}$ with a world average [11] in that scheme. It turns out that $m_{\rm res} \simeq 0.5$ MeV at $a^{-1} \simeq 2.4$ GeV with $N_5 = 12$. At $a^{-1} \simeq 3.6$ GeV, $m_{\rm res}$ is even smaller ($\simeq 0.1$MeV) with smaller $N_5 = 8$. While these $m_{\rm res}$'s are already much smaller than $m_{ud,\rm phys}$, we are considering to further reduce $m_{\rm res}$ by reweighting [12].

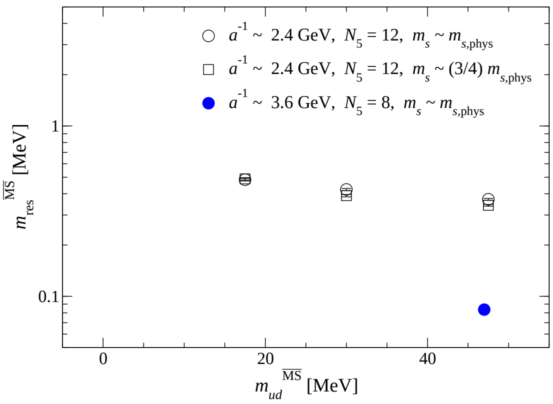

Figure 5: $m_{\rm res}$ in $\overline{\rm MS}$ scheme at 2 GeV.

In Fig. 6, we compare the topological tunneling at $a^{-1} \sim 2.4$ and 3.6 GeV. The auto-correlation largely increases by approaching the continuum limit with the unit trajectory length τ held fixed. As suggested in Ref. [13], we observe that topology changes more frequently with larger τ in our study in quenched QCD at a similar cut-off $a^{-1} \simeq 3.5$ GeV. This observation leads us to increase τ when exploring a^{-1} above 2.4 GeV to accelerate our Monte Carlo sampling of topological sectors.

In this article, we reported on our new project of large-scale simulations of $N_f = 2+1$ QCD with good chiral symmetry. The lattice action is chosen by the comparative study to reduce $m_{\rm res}$ well below the physical quark masses and achieve a factor of 20 acceleration compared to the overlap formulation. We are planning to accumulate high statistics of 10,000 MD time for a precision study

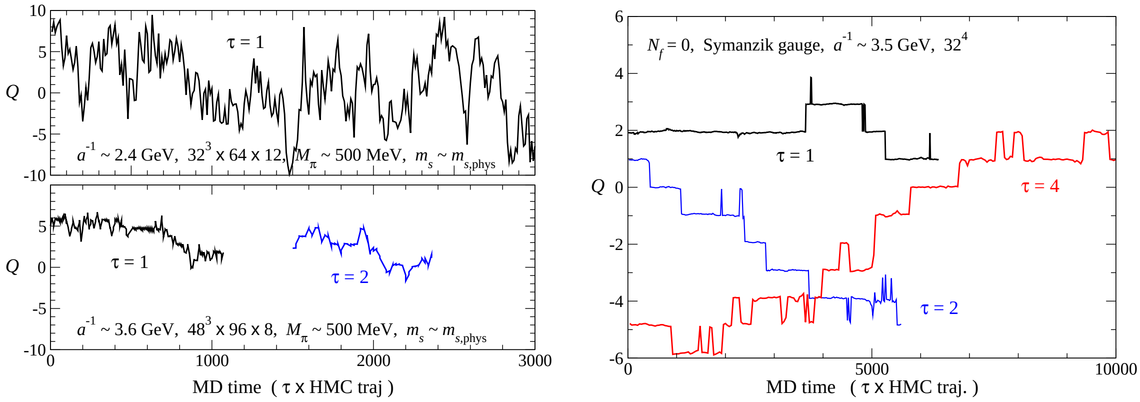

Figure 6: Left panels: Monte Carlo history of topological charge Q in our simulations of $N_f = 2+1$ QCD at $a^{-1} \simeq 2.4$ (left-top panel) and 3.6 GeV (left-bottom panel). Right panel: history of Q in our study in quenched QCD at $a^{-1} \simeq 3.5$ GeV with different values of τ.

of QCD. Our preliminary results on the light hadron physics were presented at this conference [14].

Numerical simulations are performed on Hitachi SR16000 and IBM System Blue Gene Solution at High Energy Accelerator Research Organization (KEK) under a support of its Large Scale Simulation Program (No. 12/13-04). This work is supported in part by the Grants-in-Aid for Scientific Research (No. 21674002, 25287046), the Grant-in-Aid for Scientific Research on Innovative Areas (No. 2004: 20105001, 20105002, 20105003, 20105005, 23105710), and SPIRE (Strategic Program for Innovative Research).

References

[1] S. Aoki *et al.* (JLQCD and TWQCD Collaborations), Prog. Theor. Exp. Phys., 01A106 (2012). See also X. Feng, PoS **LATTICE 2013**, 008; X. Feng *et al.*, *ibid.*, 480; T. Iritani *et al.*, *ibid.*, 376 (in these proceedings).

[2] R.C. Brower, H. Neff and K. Orginos, Nucl. Phys. (Proc.Suppl.) **140**, 686 (2005); arXiv:1206.5214 [hep-lat].

[3] C. Morningstar and M. Peardon, Phys. Rev. D **69**, 054501 (2004).

[4] C. Aubin *et al.* (MILC Collaboration), Phys. Rev. D **70**, 094505 (2004).

[5] S. Hashimoto *et al.* (JLQCD Collaboration), PoS **LATTICE 2013**, 431 (in these proceedings).

[6] Y-G. Cho *et al.* (JLQCD and UKQCD Collaborations), PoS **LATTICE 2013**, 255 (in these proceedings).

[7] M. Hasenbusch, Phys. Lett. B **519**, 177 (2001).

[8] I. Horváth, A.D. Kennedy and S. Sint, Nucl. Phys. (Proc.Suppl.) **73**, 834 (1999).

[9] I.P. Omelyan, I.M. Mryglod and R. Folk, Phys. Rev. E **65**, 056706 (2002); T. Takaishi and P. de Forcrand, Phys. Rev. E **73**, 036706 (2006).

[10] G. Cossu *et al.* (JLQCD Collaboration), PoS **LATTICE 2013**, 482 (in these proceedings).

[11] G. Colangelo *et al.* (FLAG working group of FLAVIANET), Eur. Phys. J. C **71**, 1695 (2011).

[12] H. Fukaya *et al.* (JLQCD Collaboration), PoS **LATTICE 2013**, 127 (in these proceedings).

[13] S. Schäfer, R. Sommer, F. Virotta (ALPHA Collaboration), Nucl. Phys. B **845**, 93 (2011); Lüscher and Schäfer, JHEP **1107**, 036 (2011).

[14] J. Noaki *et al.* (JLQCD Collaboration), PoS **LATTICE 2013**, 263 (in these proceedings).